ASIAN JOURNAL OF ERGONOMICS, 2002, 3(2), 83-104

A 3-D Craniofacial Anthropometric Database - with an Application for Design of Full-Face Respiratory Masks

Yi-Hsueh Yang†, Chi-Yuang Yu
Department of Industrial Engineering,
National Tsing Hua University,
101 Sec. 2, Kuang-Fu Rd.,
Hsinchu 300, Taiwan, ROC

This study established a 3-D craniofacial anthropometric database and applied it to the design respiratory masks. A 3-D photo-grating measuring system, which scans more than 100,000 3-D surface points in 94 seconds, was used to measure craniofaces. The database consisted of 1213 subjects, randomly selected from the Taiwanese worker population, but adjusted for gender and age group distribution. This database was used to extract 39 1-D measurements and select three 3-D head models for the design of respiratory masks. These 1-D measurements were calculated from a set of 24 anatomic landmarks, of which 16 were identified automatically and 8 were identified manually. These three 3-D head models are intended to represent the small, medium and large size groups, which fit best the whole population. The 3-D head models were processed by sizing and selection procedures. The sizing procedure was to group the data into three size groups by optimizing the dispersion of the face length and face breadth against allowable design tolerance. The selection procedure was to select a "typical model" within each size group using the form-difference analysis technique. The typical model had the smallest form-difference value within the group. Finally, these three 3-D head models were made by a computerized numerical control machine (CNC) and used for the design of respiratory masks.

Key words: 3-D anthropometry, head models, mask design, mask air-tightness

1. INTRODUCTION

The objective of this study was to establish a 3-D craniofacial anthropometric database and apply it to the design of respiratory masks. In Taiwan, the demand for adequately designed respiratory masks has not been properly met. According to a report of the Council of Laborers' Affairs (1994a, 1994b), about 840,000 workers, or approximately 14.71% of the work population, needed to wear respiratory masks

† *Corresponding author:* yyx318@ms24.hinet.net

while working. Furthermore, statistics on laborer insurance compensation also showed that a total of 682 cases of pneumoconiosis between 1985 and 1993 were possibly caused by wearing improper respiratory masks (Bureau of Laborer Insurance, 1993). The problem lies in the fact that most masks available in Taiwan, whether imported or made domestically are designed primarily for foreigners rather than Taiwanese workers. Taiwanese have craniofaces that are clearly quite different from foreigners, in both size and shape (Molnar, 1992; Yu et al., 1996; Boaz and Almguist, 1997), resulting in severe mask leakage problems when Taiwanese use masks designed for foreigners.

Mask leakage is mainly due to a poor fit at the interface between the mask and the face (Olestenstad and Perkin, 1990; Olestenstad et al., 1992). The problem arises because (1) the surface of the face has a highly complex 3-D form; (2) faces vary in size and shape. Therefore, designing a mask that perfectly fits the complex face is difficult, and designing a limited number of mask sizes to fit the entire population is even more challenging. Case et al. (1989) noted that mask mismatch was caused by the lack of 3-D anthropometric facial data. Therefore, a 3-D database of precise facial shapes and sizes is a basic requirement for tackling this problem.

As a consequence, this study was undertaken to establish an indigenous 3-D craniofacial anthropometric database. Its major objective was to apply detailed 3-D size and form information to the design of respiratory masks so that a better man-machine fit could be achieved; and its secondary objective was to extract traditional 1-D measurements in a more automatic fashion.

2. METHODS

A 3-D photograting measurement system was developed and used for the measurement of craniofaces. This study established a database containing 1190 subjects, which were chosen from the Taiwanese working population, and adjusted for gender and age group distribution. When the database was established, it was used to extract 39 traditional 1-D measurements and select three 3-D head models for designing respiratory masks.

2.1. Sampling

A sample including 1190 subjects of mixed genders was selected from the Taiwanese working population of 6.26 million. The sample size was intended to yield estimates of both face length and face breadth to within a 0.5 mm maximal allowable error. This maximal allowable error was a compromise between the sponsor and the investigators under the consideration of ideal and reality. The face length is defined as the menton-sellion length and the face breadth as the bizygomatic breadth (NASA, 1978). Table 1 lists the face length and face breadth statistics of similar racial groups, six males and one female (NASA, 1978; PROC, 1981). The largest standard deviation is 8.8 mm (face breadth of Japanese Airforce), and a sample size of 1190 is required to yield 95% confidence. This sampling was also intended to yield a sample distribution in gender and age groups (18-24, 25-39, 40-54, and 55+) similar to that of the entire population. Table 2 lists the age and gender distribution of the population, and the expected sizes of the samples to be drawn. The expected male sample size was 702 (by age group, 96, 364, 189 and 52), while that of females was 488 (by age group, 119, 246, 108 and 15).

A modified three-phase sampling for stratification was used, following the structure profession, company, and worker (Cochran, 1977). The first phase was proportional allocation in stratified sampling, which drew 16 professions out of a total of 67 (approximately 25%) listed in the Taiwan Human Resource Report (Directorate-General of Budget, Accounting and Statistics Executive Yuan, 1991). The numbers of subjects drawn from each profession was based on the ratio of workers in that profession compared to the total workers in the 16 professions selected. The second phase was probability sampling, which drew several companies from each profession. The third phase was random sampling, which randomly drew workers from each company. The maximum number of workers drawn from a single company was 25% of the company's population.

Table 1 The Face Lengths and Face Breadths in mm of Seven Asian Racial Groups Listed in Webb Associates (1978) and PROC (1981)

Database	*Sample Size (N)*	*Gender*	*Face Length*		*Face Breadth*	
			Mean	*S.D.*	*Mean*	*S.D.*
Japanese Airforce	1,176	M	n.a.	n.a.	122.7	8.8
Japanese Pilots	236	M	121.0	5.8	143.0	6.3
Thai Military	2,950	M	114.0	6.0	131.0	7.0
Vietnam Military	2,128	M	113.2	6.0	127.7	5.9
Korean Force	3747	M	116.0	5.0	143.0	6.0
Chinese Males	11,164	M	125.8	n.a.	119.0	n.a.
Chinese Females	1,115	F	144.5	n.a.	139.0	n.a.

Note: n.a. means that the data is not available.

Table 2 The Distribution in Gender and Age Group of Taiwanese Workers Population and Expected Sample to be Drawn

Sample		*Gender*		*Age Group*			
				18-24	*25-39*	*40-54*	*55+*
Population (6,260,000)		Male	3,691,000	503,000	1,917,000	996,000	275,000
			58.96%	8.04%	30.62%	15.91%	4.39%
		Female	2,569,000	628,000	1,292,000	568,000	81,000
			41.04%	10.03%	20.64%	9.07%	1.29%
Expected Sample	(1,190)	Male	702	96	364	189	52
			58.96%	8.04%	30.62%	15.91%	4.39%
		Female	488	119	246	108	15
			41.04%	10.03%	20.64%	9.07%	1.29%

Table 3 The Gender and Age Group Distribution in Expected Sample and Resultant Sample

Sample		*Gender*		*Age Group*			
				18-24	*25-39*	*40-54*	*55+*
Expected Sample	(1,190)	Male	702 58.96%	96 8.04%	364 30.62%	189 15.91%	52 4.39%
		Female	488 41.04%	119 10.03%	246 20.64%	108 9.07%	15 1.29%
Resultant Sample	(1,213)	Male	717 59.11%	100 8.24%	376 31.00%	189 15.58%	52 4.29%
		Female	496 40.89%	123 10.14%	252 20.77%	107 8.82%	14 1.15%

2.2. 3D Photograting Measurement System

The 3-D photograting system consists of six liquid crystal device (LCD) projectors, four charge couple device (CCD) cameras, three controllers, a PC and an auxiliary graphical monitor (Figure 1). The LCD projects a series of grating patterns on the cranioface, and the CCD camera scans this image. The image is then used to calculate 3-D coordinates of the surface points on the cranioface, using triangulation and Gray coding methods (Lou, 1992). The LCD projectors and the CCD cameras were installed on a double-layer "L-type" structure, with each layer of the "L-type" structure being made of two square 200cm long aluminum beams, perpendicularly and horizontally connected to each other.

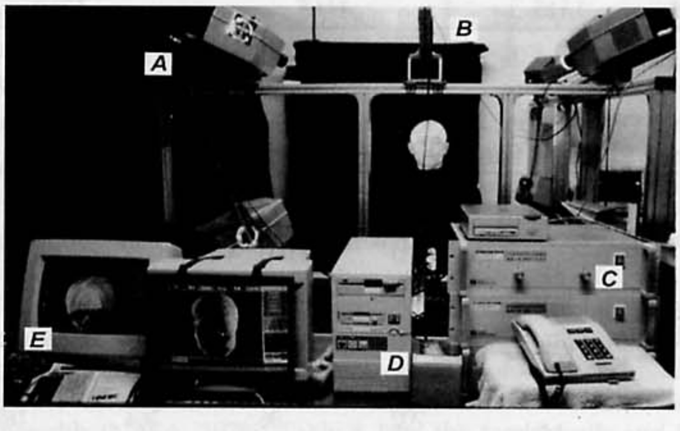

Figure 1 The 3-D photograting measurement system consists of six liquid crystal device (LCD) projectors (A), four charge couple device (CCD) cameras (B), three controllers (C), a PC (D) and an auxiliary graphical monitor (E).

Three LCD projectors and two CCD cameras were installed on the upper layer, and the remainders were installed on the lower layer. All of the six LCD projectors and four CCD cameras were appropriately slanted and adjusted so that all of their photo axes pointed to the geometric center of the structure, where the cranioface was to be positioned. Each CCD camera scanned two images, one was projected from the LCD projector to the right, and the other to the left. In all, four CCD cameras took a total of eight regional measurements in various directions (Figure 2). An area in the right posterior region behind the ear, where it is blocked by the head support fixture, is unmeasured. This unmeasured area was made up by mirror imaging afterward. These eight regional measurements were finally integrated as a single file. The final file consists of approximately 100,000 surface points.

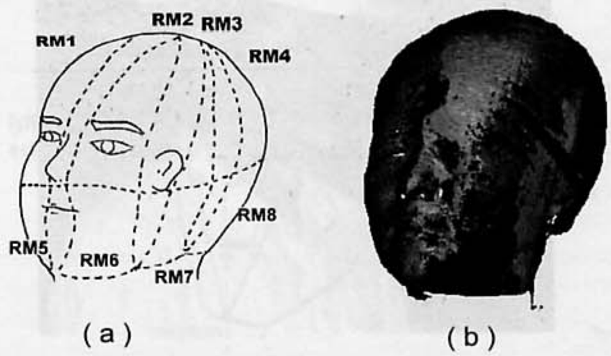

Figure 2 The measurement result of the 3-D photograting measurement system. (a) The eight regional measurements taken from different directions are RM1 to RM8. (It is noted that these regional measurements are overlapped.) (b) The eight regional files are shown in different colors.

The system was tested for precision and accuracy, the precision was to evaluate the repeatability of the system among repetitive measures, and the accuracy was to compare its measurement with a selected true standard. The test apparatus was a white helmet to which 12 black markers with diameters of 15mm were attached (Figure 3). The precision test was to compute the dispersions of these 12 markers among ten repetitive measurements, and showed that the dispersion ranged from 0.46 mm to 0.88 mm, with a mean of 0.62 mm (S.D.=0.14 mm). Meanwhile, the accuracy test was to compare the displacement error of the 12 markers measured by this photograting measurement system with the digital readout of the sliding gauge (Mitutoyo CD-6, accuracy: 0.01 mm) on which the helmet was assembled. The sliding gauge was randomly positioned in five directions and slid by 200 mm. The accuracy test showed that errors among 10 repetitive measurements ranged between 0.80 mm and 1.43 mm, with a mean of 0.75 mm (S.D.=0.22 mm). Both the precision test and accuracy tests showed that this photograting measurement system is far better than the measurement devices used for traditional anthropometry (see Discussion).

A postural stabilizer was used to stabilize the subject during measurement. The postural stabilizer was fabricated from an adjustable hydraulic jack, a car seat and a head support fixture. Both the car seat and the head support fixture were three-way adjustable, allowing the craniofaces of differently sized subjects to be positioned exactly at the geometrical center of the structure.

Figure 3 The white helmet was used for precision and accuracy tests. It was attached with 12 black markers of 15mm in diameter.

2.3. Measurement Procedure

Before measurement, the subject was asked to wear a white swimming cap and apply white powder to the eyebrows and, for male subjects, the mustache area. The white cap and powder were intended to press the hair as close to the skin as possible, and to increase the contrast of the grating lines.

During measurement the subject was asked to sit on the postural stabilizer, and was then restrained by two seat belts and had his/her head supported by the head support fixture. The ambient light was then turned off, and the subject was asked to close the eyes and hold their posture for measurement. The measurement time was 94 seconds. An on-site checking immediately followed the completion of the measurement. This checking ensured that postural movement during measurement was less than 2 mm, and involved visually examining the mismatch of the overlapping areas among eight regional measurements. The measurement was repeated, if any problems were found.

The measurement data were then transformed into a head-based coordinate system. This was because the orientation of the head differed between subjects during measurement, and this needed to be aligned before subsequent data analyses. The alignment proceeded by rotating each cranioface to a head-based coordinate system based on three facial landmarks. Three prominent anatomical landmarks, namely the right and left outer corners of the eye and the menton were identified as reference points (Figure 4). The line connecting the two outer corners of the eye was designated as the X-axis, and the middle point between the two outer corners of the eye was defined as the origin of the head's coordinates. The line connecting the origin to the menton was the Y-axis.

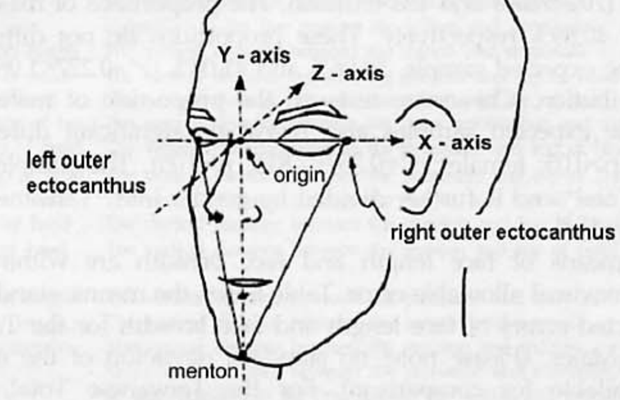

Figure 4 The head-based coordinates system used for the alignment of different craniofaces. The line connecting the left and right outer corner of the eye is designated as X-axis, and the middle point between these two outer corners of the eye is defined as the origin. The line connecting the origin and menton is Y-axis.

2.4. Data Analyses

After measurements were completed, 39 1-D measurements were extracted and three 3-D head models were selected for design references. (The analyses for the selection of three 3-D head models are included along with the presentation of the results, and are therefore described in the Results Section.) These 39 1-D measurements, consisting of 31 distances and eight arc lengths are listed in Table 4, and part of them are illustrated in Figure 5. The distance is defined as one of three distances between two designated anatomical landmarks: vertical distance, horizontal distance or oblique distance. And arc length is defined either as a circumference or an arc length passing three designated anatomical landmarks, simulating as being measured with a tape measure. These 39 1-D measurements were automatically computed from a pool of 24 anatomical landmarks. Among these 24 landmarks, eight were identified manually (either semi-automatically, or

Table 4 The Definitions of the 39 1-D Measurements

Measurement	*Definition*	*Distance/ Arc length*
1 Menton-sellion length (Face length)	The vertical distance between the menton and sellion.	Distance
2 Bizygomatic breadth (Face breadth)	The breadth between the left and right zygomatic.	Distance
3 Head breadth	The breadth between the left and right widest point of head.	Distance
4 Bitragion breadth	The breadth between the left and right tragion.	Distance
5 Biocular breadth	The breadth between the left and right outer ectocanthus.	Distance
6 Interocular breadth	The breadth between the left and right inner ectocanthus.	Distance
7 Nasal breadth	The breadth between the left and right side of nose.	Distance
8 Lip length	The breadth between the left and right corner of mouth.	Distance
9 Nose length	The oblique distance between the sellion and subnasale, in parallel to the line passing the sellion and pronasale.	Distance
10 Subnasal - sellion length	The vertical distance between the sellion and subnasale.	Distance
11 Glabella to top of head	The vertical distance between the glabella and top of head.	Distance
12 Sellion to top of head	The vertical distance between the sellion and top of head.	Distance
13 Ectocanthus to top of head	The vertical distance between the outer ectocanthus and top of head	Distance
14 Pronasale to top of head	The vertical distance between the pronasale and top of head	Distance
15 Subnasale to top of head	The vertical distance between the subnasale and top of head	Distance
16 Tragion to top of head	The vertical distance between the tragion and top of head	Distance
17 Stomion to top of head	The vertical distance between the stomion and top of head	Distance
18 Menton to top of head (Head length)	The vertical distance between the menton and top of head	Distance
19 Pronasale-menton length	The vertical distance between the pronasale and menton.	Distance
20 Menton-subnasle length	The vertical distance between the menton and subnasle.	Distance
21 Stomion-menton length	The vertical distance between the stomion and menton.	Distance
22 Nose protrusion	The oblique distance between the pronasale and subnasale, in perpendicular to the line passing the sellion and pronasale.	Distance
23 Pronasle-tragion length	The distance between the pronasale and tragion.	Distance
24 Sellion to wall	The horizontal distance from the sellion to wall.	Distance
25 Ectocanthus to wall	The horizontal distance from the outer ectocanthus to wall.	Distance
26 Pronasale to wall	The horizontal distance from the pronasale to wall.	Distance
27 Subnasale to wall	The horizontal distance from the subnasale to wall.	Distance
28 Glabella to wall (Head depth)	The horizontal distance from the glabella to wall.	Distance
29 Stomion to wall	The horizontal distance from the stomion to wall.	Distance
30 Tragion to wall	The horizontal distance from the tragion to wall.	Distance
31 Menton to wall	The horizontal distance from the menton to wall.	Distance
32 Bitragion-crinion arc	The arc length from the right to left tragion simulating as a tape measure passing over the crinion.	Arc length
33 Bitragion-inion arc	The arc length from the right to left tragion simulating as a tape measure passing over the inion.	Arc length
34 Bitragion-menton arc	The arc length from the right to left tragion simulating as a tape measure passing over the menton.	Arc length
35 Bitragion-min. front. arc	The arc length from the right to left tragion simulating as a tape measure passing over the glabella.	Arc length
36 Bitragion-subnasale arc	The arc length from the right to left tragion simulating as a tape measure passing over the subnasale.	Arc length
37 Head circumference	The maximum circumference of the head above the glabella.	Arc length
38 Glabella-head circum.	The circumference of the head passing the glabella	Arc length
39 Glabella-inion arc	The arc length simulating as a tape measure passing over the glabella and subnasale.	Arc length

Note: Among them, 31 are distances and eight are arc lengths. The anatomically landmarks used in defining these measurements are listed (with identification methods) in Table 5.

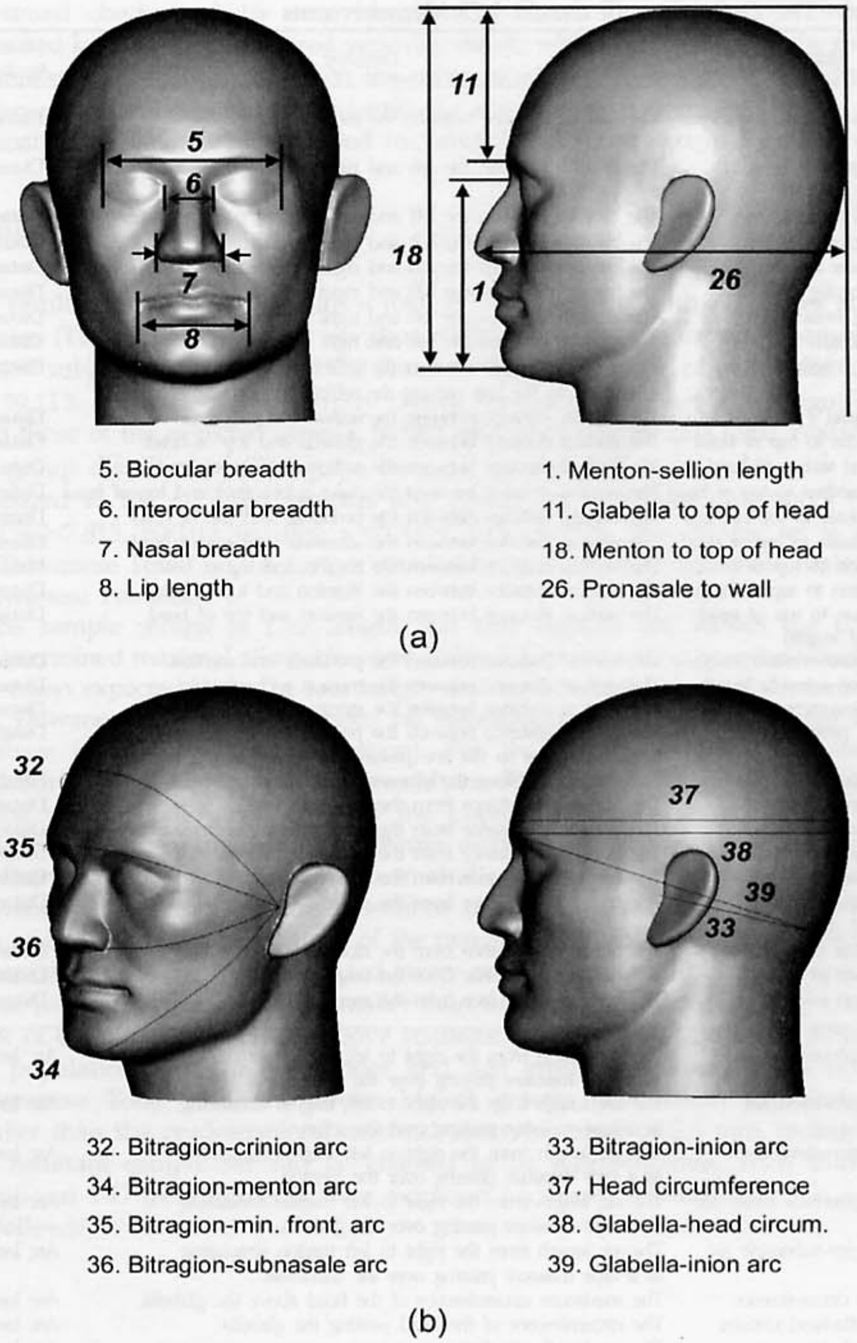

Figure 5 Illustrations of a part of the 39 1-D measurements extracted in this study, (a) eight distances. (b) eight arc lengths.

Table 5 The Identification Methods of the 24 Anatomical Landmarks Used to Extract the 39 1-D Measurements Listed in Table 4

	Landmark	*Identification Method*	*Automatic/ Manual*
1	Left inner ectocanthus	The inner end of the left eyelid opening.	Manual
2	Right inner ectocanthus	The inner end of the right eyelid opening.	Manual
3	Left outer ectocanthus	The outer end of the left eyelid opening.	Manual
4	Right outer ectocanthus	The outer end of the right eyelid opening.	Manual
5	Left side of nose	The point on the left most wing of nose.	Manual
6	Right side of nose	The point on the right most wing of nose.	Manual
7	Left tragion	The point on the left tragion.	Manual
8	Right tragion	The point on the right tragion..	Manual
9	Top of head	The highest point on the mid-sagittal cross-sectional contour of the head.	Automatic
10	Crinion (Hair line)	The middle point (in height) between the top of head and glabella on the mid-sagittal cross-sectional contour of the head.	Automatic
11	Glabella	The most protruding point between the top of head and sellion on the mid-sagittal cross-sectional contour of the head.	Automatic
12	Sellion	The most concave point in range between pronasale and a point 6 cm above on the mid-sagittal cross-sectional contour of the head.	Automatic
13	Pronasale	The most protruding point on the mid-sagittal cross-sectional contour of the head.	Automatic
14	Subnasale	The most concave point in range between pronasale and a point 2 cm below on the mid-sagittal cross-sectional contour of the head.	Automatic
15	Stomion	The most concave point in range between subnasale and a point 4 cm below on the mid-sagittal cross-sectional contour of the head.	Automatic
16	Menton	The point whose tangent is 45o below the stomion on the mid-sagittal cross-sectional contour of the head.	Automatic
17	Left widest point of head	The left most point by searching through all the horizontal cross-sectional contours above sellion.	Automatic
18	Right widest point of head	The right most point by searching through all the horizontal cross-sectional contours above sellion.	Automatic
19	Left zygomatic	The left point whose tangent is 75o to the coronal plane on the horizontal cross-sectional contour passing through the mid-nasal point. The mid-nasal is the middle point between pronasale and sellion	Automatic
20	Right zygomatic	The right point which is similar to no. 19	Automatic
21	Left corner of mouth	The left end of the lip opening. The lip opening is the fitted line of a series of longitudinal discontinuity points searched within a 3 cm (height) by 6 cm (width) rectangular whose center is 3 cm below the subnasale.	Automatic
22	Right corner of mouth	The right end of the lip opening. (Similar to no. 21)	Automatic
23	Back of head	The most protruding posterior point on the mid-sagittal cross-sectional contour of the head.	Automatic
24	Inion	The middle point in range between an arc segment on the posterior aspect of mid-sagittal cross-sectional contour of the head. The top end point of this arc segment is at the level of the tragion and bottom end point at the level of the lowest point of the pinna.	Automatic

Note: Among them, eight are manually identified, and 16 are automatically identified.

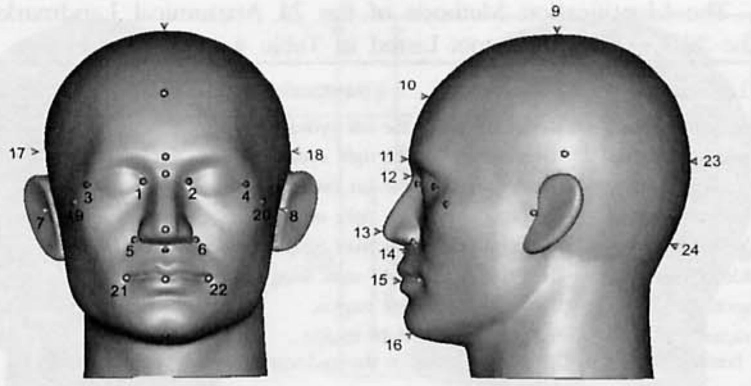

Figure 6 Illustrations of the 24 anatomical landmarks used to define the 39 1-D measurements extracted in this study.

Table 6. The Standard Deviations and Mean Expected Errors of Face Length and Face Breadth in mm of Taiwanese Total, Taiwanese Males

Measurement	*Taiwanese Total (N=1213)*			*Taiwanese Males (N=717)*		
	S.D.	*M.E.E*	*M.E.E.< 0.5*	*S. D.*	*M.E.E.*	*M.E.E.< 0.5*
Face Length	7.3	+/- 0.41	True	6.3	+/- 0.46	True
Face Breadth	7.0	+/- 0.39	True	6.6	+/- 0.48	True

Note: M. E. E stands for mean expected error and the predetermined mean expected error is 0.5 mm.

3.1. One-Dimensional Measurements

Table 7 lists the results of 39 1-D measurements of the Taiwanese Total, Taiwanese Males and Taiwanese Females groups, along with nine existing databases (NASA, 1978; PROC 1981). These nine existing databases include the Japanese Airforce, Japanese Pilots, Thai Military, Vietnam Military, Korean Forces, Chinese Males, USAF, NATO, and Chinese Females. Among these above databases, six are Asian males, two are Caucasian males and one is Asian female. Notably, Table 7 contains a large number of blank spaces. Among these databases, the USAF and NATO database consist of 28 measurements (the most), while the Thai Military, Vietnam Military and Korean Forces consist of only 5 measurements (the least).

Table 7 The Results of 39 1-D Measurements, 31 Distances and Eight Arcs in mm of Taiwanese Total, Taiwanese Males and Taiwanese Females, are Listed Along with Nine Existing Databases

	Measurement	*Taiwanese*			*Existing, Male*		
		Total N=1213	*Males* N=717	*Females* N=496	*Jap. Airforce* N=1176	*Jap. Pilots* N=236	*Thai M.* N=2950
1	**Menton-sellion length (Face length)**	**111.7 (7.3)**	**115.0 (6.3)**	**106.8 (5.9)**		**121.0 (5.8)**	**114.0 (6.0)**
2	**Bizygomatic breadth (Face breadth)**	**131.9 (7.0)**	**134.6 (6.6)**	**127.8 (5.4)**	**127.7 (8.8)**	**143.0 (6.3)**	**131.0 (7.0)**
3	**Head breadth**	**168.1 (8.9)**	**170.9 (8.4)**	**164.1 (7.9)**	**157.7 (6.0)**	**157.6 (6.1)**	**152.0 (7.0)**
4	Bitragion breadth	158.0 (9.2)	161.9 (8.2)	152.4 (7.6)	142.8 (5.4)	142.1 (6.5)	
5	Biocular breadth	106.0 (6.7)	108.1 (6.5)	102.9 (5.8)			
6	Interocular breadth	32.3 (3.6)	32.9 (3.7)	31.4 (3.3)			
7	Nasal breadth	39.2 (3.4)	40.9 (2.9)	36.9 (2.6)			
8	Lip length,	47.4 (4.5)	48.7 (4.4)	45.4 (3.7)		51.2 (4.3)	
9	Nose length	41.8 (4.2)	43.2 (3.9)	39.8 (3.8)		49.7 (3.3)	
10	Subnasal-sellion length	48.9 (3.9)	50.3 (3.6)	46.9 (3.5)			
11	Glabella to top of head	94.6 (8.5)	94.8 (8.6)	94.3 (8.3)			
12	Sellion to top of head	117.4 (9.2)	116.8 (9.2)	118.4 (9.2)			
13	Ectocanthus to top of head	120.6 (7.8)	120.2 (8.0)	121.1 (7.6)	112.4 (11.9)		
14	Pronasale to top of head	153.4 (8.6)	153.7 (8.9)	152.8 (8.1)			
15	Subnasale to top of head	166.4 (8.6)	167.1 (8.8)	165.3 (8.2)			
16	Tragion to top of head	137.4 (9.1)	137.2 (9.4)	137.8 (8.7)			128.0 (10.0)
17	Stomion to top of head	190.0 (8.8)	191.6 (8.8)	187.7 (8.2)			
18	**Menton to top of head (Head length)**	**229.1 (9.7)**	**231.8 (9.4)**	**225.1 (8.7)**	**234.2 (10.5)**		
19	Pronasale-menton length	75.7 (5.8)	78.1 (5.3)	72.3 (4.7)			
20	Menton-subnasle length	62.7 (5.3)	64.7 (4.9)	59.9 (4.4)		73.2 (4.7)	
21	*Stomion-menton length*	*39.1 (4.1)*	*40.2 (4.1)*	*37.4 (3.5)*			
22	Nose protrusion	18.4 (3.4)	18.9 (3.6)	17.6 (2.8)			
23	Pronasle-tragion length	106.2 (8.3)	110.6 (7.1)	100.0 (5.4)			
24	Sellion to wall	183.5 (9.1)	187.5 (8.0)	177.6 (7.3)			
25	Ectocanthus to wall	166.6 (8.7)	169.3 (8.1)	162.6 (8.1)			
26	Pronasale to wall	204.7 (10.3)	209.7 (8.7)	197.3 (7.9)			
27	Sub nasale to wall	192.4 (9.8)	196.9 (8.6)	186.0 (7.8)			
28	**Glabella to wall (Head depth)**	***186.7 (9.2)***	***190.8 (8.1)***	***180.8 (7.2)***			
29	Stomion to wall	192.6 (10.0)	196.9 (8.8)	186.4 (8.2)			
30	*Tragion to wall*	*98.4 (8.3)*	*99.2 (8.8)*	*97.4 (7.5)*	*95.2 (7.6)*		
31	Menton to wall	183.5 (9.1)	187.5 (8.0)	177.6 (7.3)			
32	Bitragion-crinion arc	315.3 (17.2)	320.4 (16.7)	308.0 (15.3)			
33	Bitragion-Inion arc	277.2 (17.4)	279.0 (18.2)	274.7 (15.8)			
34	Bitragion-menton arc	318.9 (20.4)	329.5 (17.7)	303.6 (13.0)		319.6 (12.1)	
35	Bitragion-min. front. arc	285.7 (16.8)	293.8 (14.9)	274.1 (12.0)	314.2 (12.0)	316.0 (11.0)	
36	Bitragion-subnasale arc	283.1 (16.8)	291.2 (15.4)	271.5 (10.7)	297.7 (11.9)		
37	**Head circumference**	**569.3 (24.3)**	**581.6 (20.1)**	**551.6 (18.0)**	**563.3 (13.9)**	**563.8 (14.8)**	**540.0 (14.0)**
38	Glabella-head circum.	569.1 (24.5)	581.3 (20.4)	551.4 (18.2)			
39	Glabella-inion arc	560.9 (22.0)	571.5 (19.4)	545.7 (15.8)			
	Number of Measurement	39	39	39	9	10	5

Note: Numbers are average values with standard deviations in parenthesis and the measurements in bold face type are used for comparison among databases.

(Continue)

Measurement	*Existing, Male Exist., Female*					*Female*
	Vietnam M. N=2128	*Korean F. N=3747*	*China Male N=11164*	*USAF N=3869*	*NATO N=3325*	*China N=1115*
1 Menton-Sellion Length (Face Length)	113.2 (6.0)	116.0 (5.0)	125.8	119.2 (6.8)	119.7 (5.9)	119.0
2 Bizygomatic Breadth (Face Breadth)	127.7 (5.9)	143.0 (6.0)	144.5	139.9 (5.6)	142.4 (5.3)	139.0
3 Head Breadth	149.0 (5.8)	153.0 (6.0)	154.1	153.1 (5.8)	155.5 (6.0)	149.1
4 Bitragion Breadth			142.6	138.5 (6.5)	144.9 (5.3)	136.6
5 Biocular Breadth			92.6	94.2 (5.3)	91.0 (3.9)	90.5
6 Interocular Breadth			36.6	31.5 (2.8)	32.9 (2.6)	35.8
7 Nasal Breadth			38.9	34.2 (3.8)	36.2 (2.6)	36.1
8 Lip Length,			50.4	48.7 (4.4)	51.4 (3.4)	47.7
9 Nose Length			57.9			54.7
10 Subnasal-Sellion Length			57.9	51.0 (3.7)	52.5 (3.4)	54.7
11 Glabella to Top of Head				92.1 (8.1)	88.0 (8.4)	
12 Sellion to Top of Head				108.4 (7.8)	105.3 (7.9)	
13 Ectocanthus to Top of Head				115.9 (6.7)	113.9 (7.4)	
14 Pronasale to Top of Head				148.3 (8.7)	146.8 (9.4)	
15 Subnasale to Top of Head						
16 Tragion to Top of Head	123.3 (7.8)	125.0 (8.0)		131.8 (6.2)	131.8 (5.9)	
17 Stomion to Top of Head				182.3 (8.4)	179.3 (8.5)	
18 Menton to Top of Head (Head length)			229.3	226.7 (9.7)	224.5 (8.9)	221.5
19 Pronasale-Menton Length						
20 Menton-Subnasle Length			69.1	70.1 (6.1)	68.5 (5.0)	64.3
21 Stomion-Menton Length						
22 Nose Protrusion			18.1	23.5 (3.0)	23.3 (2.6)	16.8
23 Pronasle-Tragion Length						
24 Sellion to Wall				196.0 (7.0)	191.0 (7.6)	
25 Ectocanthus to Wall				172.1 (7.4)	167.3 (7.3)	
26 Pronasale to Wall				219.8 (8.2)	216.4 (8.3)	
27 Sub nasale to Wall						
28 Glabella to Wall (Head Depth)			187.8	198.0 (7.1)	193.6 (7.8)	178.6
29 Stomion to Wall						
30 Tragion to Wall				96.3 (6.8)	92.8 (6.4)	
31 Menton to Wall						
32 Bitragion-Crinion Arc						
33 Bitragion-Inion Arc						
34 Bitragion-Menton Arc				314.1 (14.4)	321.2 (12.5)	
35 Bitragion-Min. Front. Arc				304.8 (11.1)	302.4 (10.7)	
36 Bitragion-Subnasale Arc				287.0 (11.7)	287.4 (10.6)	
37 Head Circumference	540.7 (14.1)	544.0 (13.0)		562.6 (16.5)	558.6 (15.5)	
38 Glabella-Head-Circum.						
39 Glabella-Inion Arc						
Number of Measurement	5	5	14	27	27	14

Note: Numbers are average values with standard deviations in parenthesis.

Table 7 also presents a comparison between Taiwanese Males and other male databases for six key measurements. These six measurements selected for comparison are commonly available in most of the databases. They are menton-sellion length (face length), bizygomatic breadth (face breadth), head breadth, menton-top of head (head length), glabella-wall (head depth) and head circumference (bold typed in Table 7).

1. Face length: Taiwanese Males have an average face length of 115.0 (with a SD of 6.3), similar to that of five similar Asian racial groups except for Chinese Males, and ranging between Vietnam Military 113.2 (with a SD of 6.0) and Japanese Pilots 121.0 (with a SD of 5.8), and two Caucasian racial groups USAF 119.2 (with a SD of 6.8) and NATO 119.7 (with a SD of 5.9). The differences are all within 10 mm except for Chinese Males 125.8 (no S.D).

2. Face breadth: Taiwanese Males have an average face breadth of 134.6 (with a SD of 6.6), and the comparison results are similar to those for face length with the differences all being within 10 mm except for Chinese Males at 144.5 (no S.D).

3. Head breadth: Taiwanese Males have an average head breadth of 170.9 (with a SD of 8.4), at least 13.2 mm larger than of six Asian and two Caucasian groups, and ranging between the Vietnamese 149.0 (with a SD of 5.8) and Japanese Airforce 157.7 (with a SD of 6.0).

4. Head length: Taiwanese Males have an average head length of 231.8 (with a SD of 9.4), comparable with two available Asian groups and two Caucasian groups, and ranging between NATO 224.5 (with a SD of 8.9) and Japanese Airforce 234.2 (with a SD of 10.5).

5. Head depth: Taiwanese Males have an average head depth of 190.8 (with a SD of 8.1), which is comparable with one available Asian groups and two Caucasian groups, and ranging between the Chinese Males 187.8 (no S.D.) and the USAF 198.0 (with a SD of 7.1) groups.

6. Head circumference: Taiwanese Males have an average head circumference of 581.6 (with a SD of 20.1), and similar to head breadth, this value is at least 17.8 mm larger than the five available Asian and two Caucasian groups, and ranges between the Thai Military 540.0 (with a SD of 14.0) and Japanese Pilots 563.8 (with a SD of 14.8) groups.

The Taiwanese Females and Chinese Females groups are also compared using a similar method to that above. Among the five available measurements, the Taiwanese Females group has an average face length and face breadth, 106.8 (with a SD of 5.9) and 127.8 (with a SD of 5.4), respectively, that are more than 10 mm smaller than those of Chinese Females, at 119.0 (no S.D.) and 139.0 (no S.D.), respectively. Meanwhile, the Taiwanese Females group has head length and head depth, 225.1 (with a SD of 8.7) and 180.8 (with a SD of 7.2), respectively, comparable with Chinese Females at 221.5 (no S.D.) and 178.6 (no S.D.), respectively. However, the Taiwanese Females have a larger head breadth than Chinese Females, 164.1 (with a SD of 7.9) compared to 149.1 (no S.D.). The results are similar to the comparison between Taiwanese Males and Chinese Males.

From the above comparison, face length, face breadth, head length and head depth, in both Taiwanese Males and Females, are comparable with existing databases, while head breadth and head circumference appear larger than those of existing databases. The differences in head breadth and head circumference can be attributed to the thickness of hair, since the swimming cap used in this study cannot fully press hair to the skin surface, as in a traditional caliper and tape measurement.

3.2. Three-Dimensional Typical Head Models

The selection procedure was intended to select a limited number of typical head models representing different size groups, in all they will fit the maximal number of individuals of the population. This procedure was preceded by a sizing phase and a form-difference analysis phase. The sizing phase divided the whole Taiwanese Total sample set into a limited number of size groups under the constraint of allowable design tolerance. Then the form-difference analysis phase selected a "typical model" within each size group such that the mask design based on this typical model best fitted all of the individuals in the group.

3.2.1 Sizing phase. The sizing phase was determined by sample dispersion against an allowable design tolerance and the benefits of commercial production. The dispersion of the sample was based on a bi-variant plot of face length and face breadth (Hack, et. al, 1974; CEN, 1989) (Figure 7). The range of face length is 55 mm (90 mm~145 mm) and that of face breadth is 55 mm (105 mm~160 mm). The allowable design tolerance of the full-face mask is characterized by elasticity of mask material and deformation of the flesh. Based on the consultation of experts (Coblentz, 1995) and the web catalog of manufacturers (3M, 2002), three sizes of full-face mask are preferable and the tolerance was determined to be 25 mm. With this 25 mm tolerance constraint, three sizes are needed each for face length (55 mm range) and face breadth (55 mm range). In theory, a complete set of 9 sizes would be required to cover the whole sample set. However in practice, the dispersion plot (Figure 7) shows that the number of individuals in the upper left corner and lower right corner are few, and face breadth is correlated to face length (r=0.3284), so that a set of 3 sizes is preferred by concurrently taking face length and face breadth into sizing determination.

The boundaries of each of these three size groups were determined by optimization for maximal sample coverage. Based on statistical theory, the medium size, which would bear the largest sample coverage, was determined first. Meanwhile, a square block of 25mm, earlier designated as the design tolerance of face length and face breadth, was located arbitrarily near the center of the plot. This square block was moved step-wise horizontally or vertically, until it contained a maximal number of samples (e.g. block 2 in Figure 7). This block corresponded to a face length of 100 mm to 125 mm and face breadth of 120 mm to 145 mm. This medium size group covers 996 individuals, representing approximately 82% coverage. To determine the dimensions of the large size, the square block was moved step wise again in the upper right direction until an area (block 1) was found that yielded the greatest sample coverage in union with the medium size group (block 2). The large size block corresponded to a face length of 110 mm to 135 mm and face breadth of 130mm to 155mm. This large size group covers 537 individuals, representing coverage of 44%. Finally, the measurements for the small size group were determined using a similar approach, obtaining measurements of a face length of 95 mm to 120 mm and a face breadth of 110 mm to 135 mm. This small size group covers 714 individuals, representing 59% coverage. In all, these three size groups cover 1164 individuals, representing approximately 97% coverage. It should be noted that a large proportion of both the large size and small size groups are overlapped with the medium size, and even more, the small size is slightly overlapped with the large size.

Face Length (mm)	105-110	110-115	115-120	120-125	125-130	130-135	135-140	140-145	145-150	150-155	155-160	Total
140-145						1						1
135-140							1		1			2
130-135					1	2	3	2		1		9
125-130			2	2	6	16	10	6	5			47
120-125			1	8	12	34	35	17	9	3		119
115-120		2	5	12	52	73	54	37	14	5	2	256
110-115		1	14	29	72	85	75	34	13	4	1	328
105-110		2	11	34	71	68	34	16	1	1		238
100-105		1	9	27	56	44	14	3			1	155
95-100	1		7	9	19	11	4	2				53
90-95					2	3						5
Total	1	6	49	121	291	337	230	117	43	14	4	1213

Face Breadth (mm)

Figure 7 The sizing phase was determined by sample dispersion plot of face length and face breadth against allowable design tolerance. This plot is incremented at 5 mm interval, and the number in each grid is the number of samples. The design tolerance was determined to be 25 mm, it is represented by the size of the square blocks. These three size groups were determined by optimization for maximal sample coverage.

3.2.2 Form-difference analysis phase. The Form-difference analysis phase was to select a "typical model" which has the smallest form-difference value within each size group. The form-difference analysis technique started with the comparison of the form-difference between a pair of individuals. For each individual, 16 horizontal and 13 sagittal cross-sectional contours were extracted and corresponding contours were then registered and superimposed as shown in Figure 8. The weighted sum of the areas between these two contours, named "contour-difference", was computed. The areas situated in the facial area were weighted four times more than the areas behind. The sum of these 16 horizontal and 13 sagittal contour-differences was named "individual-difference", which is a measure of form-difference between two individuals. Every individual was compared with all others in the same size group. The sum of all individual-differences was called the "group-difference", which is a measure of form-difference of an individual in relation to the whole group. The individual with the smallest group-difference was selected as the "typical model".

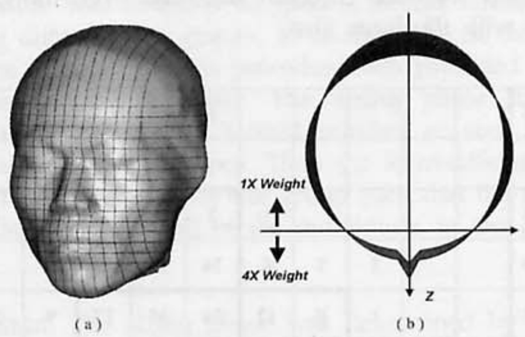

Figure 8 (a) Sixteen horizontal and 13 sagittal contour lines were extracted from each individual and used to calculate contour-difference . (b) The contour-difference is a weighted measure of the area differences between a pair of contours by superimposing on the head-based coordinates. The areas on the face are weighted four times more than the areas behind.

These typical head models from the large, medium and small size groups were fed into a computerized numerical control (CNC) machine to tool 3-D head models as shown in Figure 9.

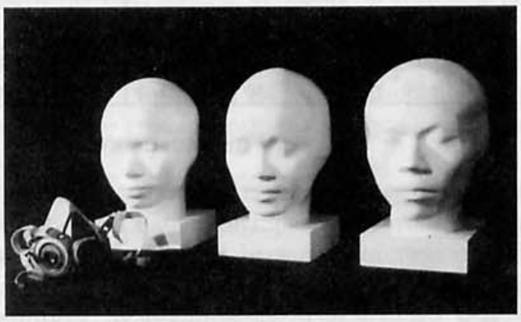

Figure 9 Three typical head models made by CNC machine.

4. DISCUSSION AND RECOMMENDATIONS

This study represents an initial attempt to demonstrate the use of 3-D anthropometric data in product design. The recent development of the 3-D human scanner allows a large 3-D anthropometric database to be collected very rapidly. Examples of such databases are the Japanese Quality Life (Kuriyama et al., 1993), the CAESAR project (Robnette et al., 1999), the SIZE UK (SIZE UK, 2000), and the SIZE USA (SIZE USA, 2002). These 3-D anthropometric databases store detailed information about bodily form, which is necessary in designing products which require a good fit to the human form, such as respiratory masks or women"s bras. However, 3-D anthropometric databases have so far been used mainly to extract traditional 1-D measurements, rather than to apply its true 3-D forms (including shape and size), because methodologies for analyzing and processing the true 3-D format have not been well explored or published. Accordingly, this study aimed not only to obtain a traditional 1-D anthropometric database, but also attempt to use the true 3-D format of the database in product design.

Three-Dimensional anthropometric data can be continuously re-used to extract all of the 1-D anthropometric measurements needed. A traditional anthropometric survey is very time consuming and costly, and the number of measurements to be taken is usually very limited. Finding a single database containing all of the measurements needed for design reference is thus very difficult. For example among the databases listed in Table 7, three contain only 5 measurements, and only two databases contain 28 measurements. In particular, some important measurements are not available, for instance, the bitragion-inion arc is needed to determine mask strap length, yet it is not included in any of the databases listed in Table 7. Initially, this study only planned to take 22 measurements, but gradually the number of measurements deemed to be necessary increased, and the final list of measurements in this study totaled 39. Later on, this database will be used again and again to extract more and more measurements for the design of other product and devices, such as a helmet, and a swimming goggle.

The 1-D measurements extracted from the 3-D anthropometric data are more consistent than traditional palpation measurements. Traditionally, landmarks were identified by in vivo palpation. Although in vivo palpation can accurately locate the landmarks of interest, it will introduce human identification error and is not consistent in repetitive measures. Some 3-D anthropometric surveys, such as CAESAR, still palpated landmarks in vivo and attached marks before measurement. However, since the 3-D anthropometric measurement itself is fully automatic, we feel that the extraction of 1-D measurements should also preferably be automatic. In a pilot study, it compared the accuracy of pre-measurement in vivo palpation with post-measurement automatic landmark identification, and revealed that the precision of automatic landmark identification with this approach was much higher than for in vivo palpation. For instance, for the zygomatic arch, the range of in vivo palpation in ten repetitive measures was 6.7 mm (with a SD of 2.7 mm). However, the range of automatic landmark identification in ten repetitive measures was only 1.7 mm (with a SD of 0.5 mm). The automatic identification algorithms considered the zygomatic arch to be the point on the cross sectional contour line passing the mid-nasal point (mid-point of nasal length) whose tangent is 800. Whether the point identified by this algorithm deviates from the true zygomatic arch has been debated, but in design practice the problem may not be serious, since the error is consistent and can be adjusted easily. For example, by varying the angle of the tangent 800 to 700, the difference was only 1.6 mm (with a SD of 0.6 mm), and to 600, was only 4.8 mm (with a SD of 2.8 mm).

The following issue must be addressed for the two procedures used for selecting the 3-D typical model, namely sizing and selection. For sizing, this study adopted face length and face breadth as the two key measurements for sizing a full-face mask, consistent with the approaches of NIOSH (Hack et. al, 1974), European Respiratory Standards (CEN, 1989), Japanese Industrial Standards (1983), Australian Standards (1984), which can be considered as standard. However, this study differs from these standards in four respects. First, these standards consider face length and face breadth independently, resulting in a set of 16 sizes (NIOSH: 4x4), and 25 sizes (Australia: 5x5). This study considered these two co-related key measurements simultaneously, thus resulting in as few as three sizes, similar to the four-size of Coblents (1991). Second, the size groups in this study are overlapping with each other, which are different from size groups in the above standards, which are mutually exclusive. Overlapping sizing seems to be more practical in the real world. For instance, for two individuals of the same body size, one may prefer to wear tight clothes, but the other may like loose ones. Personality, preference and other factors may play important roles in the fitting of a product. Third, the allowable design tolerance in the above standards is around 10 mm, while this study used 25 mm. This study used a relatively high design tolerance because new materials are highly elastic and new design configurations are more pliable and achieve a better fit on a wider range of sizes and shapes. Finally, surveys of existing product lines of full-mask makers, reveal that the number of sizes is normally less than 3.

The form-difference algorithm devised for selecting typical 3-D head models is new and requires further research. Several methods have been developed for analyzing size and shape differences in 3-D forms, such as the wavelet, fuzzy, and free form deformation (FFD) methods (Cheverud et. al, 1983; Lestrel, 1974; Mochimaru et. al, 2000a, b; Ratnaparkhi et. al, 1992). However, none of these methods can be directly applied to analyze size and shape differences for the air tightness of the face-and-mask interface. Although FFD seems to be quite promising, discrepancies exist because the degree of deformation of the control box is not a true measure of the deformation of the object. Therefore, this study considered a more direct and intuitive method. The form-difference analysis, based on the summation of weighted cross sectional differences, while not an exact measurement of air-tightness between the face and the mask, represents a direct approach to analyzing size and shape differences. Future studies will evaluate these three head models used in the design of new masks and their air-tightness. Meanwhile, a new method of generating air-tightness masks is currently under study. Hopefully more robust 3-D morphological analysis methods for evaluating face-and-mask air-tightness will be developed in the near future.

Finally, some measurements taken in the cranium region are distorted by hair thickness. This study used swimming caps to press the hair against the skin, but it was unable to fully press the hair to the skin. Consequently, measurements such as head breadth are increased at both ends by hair thickness, and head depth would add hair thickness at the posterior end. The hair thickness for men ranges approximately 2 to 8 mm, while for women it ranges from 5 to 15 mm. Although differing from traditional caliper or tape measure measurements, the above approach to measurement reflects the true measurement that must be considered in the design of respiratory masks (straps) or helmets, since hair always exists when these products are used.

REFERENCES

Australian Standards 1716, 1984. Respiratory Protective Devices, section 2. The Standard Association of Australia, North Sydney, N.S.W. Australia.

Boaz, N. T., and Almquist, A. J., 1997. Biological anthropology. Prentice Hall, New Jersey.

Bureau of Laborer Insurance, 1993. 1992 Year Statistics of Labors' Insurance Compensation in Taiwan. Bureau of Laborer Insurance, Taipei, Taiwan. (in Chinese)

Case, H., Erving, C., and Robinette, K. M., 1989. Anthropometry of a Fit Test Sample Used in Evaluating the Current and Improved MCU-2/P masks. Report AAMRL-TR-89-009, National Technical Information Service, U.S. Dept. of Commerce.

CEN European Respirator Standards EN 136, 1989. Full Face Masks for Respiratory Protective Devices. European Committee for Standardization, Brussels.

Cheverud, J., Lewis, J. L., Banchrach, W., and Lew W. D., 1983. The measurement of form and variation in form: an application of three-dimensional morphology by finite-element methods. American Journal of Physical Anthropology, 62: 341-350.

Coblentz, A., Mollard, R., and Lgnazi, G., 1991. Three-dimensional face shape analysis of French adults, and its application to the design of protective equipment. Ergonomics, 34(4): 497-517.

Coblentz, A., 1995. Personal contact, in Taipei.

Cochran, W., 1977. Sampling Techniques. 3rd edition, John Wiley & Sons.

Council of Laborers' Affairs, 1994a. Survey of Work Environmental Safety and Health Condition in Taiwan. Council of Laborers" Affairs, Taipei, Taiwan. (in Chinese)

Council of Laborers' Affairs, 1994b. 1993 Year Report of Labor Inspection. Council of Laborers" Affairs, Taipei, Taiwan. (in Chinese)

Directorate-General of Budget, Accounting and Statistics Executive Yuan, 1991. Taiwan Human Resource Report. Executive Yuan Taipei, Taiwan. (in Chinese)

Hack, A., Hyatt, E. C., Held, B. J., Moore, T. O., Richards, C.P., and Mcconville, J. T., 1974. Selection of Respirator Test Panels Representative of U.S. Adult Facial Sizes. NOISH, Cincinnati, Ohio.

Japanese Industrial Standards, T 8159, 1983. Leakage rate testing method for face pieces of respirators. Human Engineering, Tokyo, Japan. (in Japanese)

Kuriyama, H., Suguyama, Y., Ikusawa, Y. Takahasi, M., and Kato, M., 1993. Towards the Construction of A Database for Human Body Shape. Research Institute of Human Engineering for Quality Life.

Lestrel, P., 1974. Some problems in the assessment of morphological size and shape differences. Physical Anthropology, 18: 140-162.

Lou, W. S., 1992. Calibration of 3-D scanning system. Optic-Electronic Information, 23: 7-10, Institute of Industrial Technology and Research, HsinChu, Taiwan. (in Chinese)

Mochimaru, M., and Kouchi, M., 2000a. Statistics for 3-D human body forms. SAE Digital Human Modeling for Design and Engineering 2000, 2000-01-2149.

Mochimaru, M., Kouchi, M., and Dohi, M., 2000b. Analysis of 3-D human foot forms using the free deformation method and its application in grading shoe lasts. Ergonomics, 43(9): 1301-1313.

Molnar, S., 1992. Human Variation, Races, Types, and Ethnic Groups. 3rd edition, *Prentice Hall, New Jersey.*

National Aeronautics and Space Administration (NASA), 1978. Anthropometric Source Book-Volume II: A Handbook of Anthropometric Book. Webb Associates, Yellow Springs, Ohio.

Oestenstad, R. K., and Perkin, L. L., 1992. An assessment of critical anthropometric dimensions for predicting the fit of a half-mask respirator. Journal of American Industrial Hygiene Association, 53(10): 639-644.

Oestenstad, R. K., Dillion, H. K., and Perkins, L. L., 1990. Distribution of face seal leak sites on a half-mask respirator and their association with facial dimensions. Journal of American Industrial Hygiene Association, 51(5): 285-290.

Peoples Republic of China (PROC), 1981. Series of Chinese Adults" Head Form. Institute of Chinese Standards, Peking, China. (in Chinese)

Ratnaparkhi, M. V., Ratnaparkhi, M. M., and Robinette, K. M., 1992. Size and shape analysis techniques for design. Applied Ergonomics, 23(3): 181-185.

Robnette, R. M., Daanen, H., and Paquet, E., 1999. The Caesar Project: a 3-D surface anthropometry survey. 3DIM"99 Proceedings of Second International Conference on 3-D Digital Imaging and Modeling, pp. 380-386.

Yu, C. Y., Yeh W. Y., Yang, Y. X., and Chang P. H., 1996. The study for workers" typical craniofacial manikins: the establishment of Taiwan workers" craniofacial database and typical headforms. Quarterly Publication of Labors" Safety and Health Research, 4(2): 31-45, Taipei, Taiwan. (in Chinese)

3M, 2002.http://www.3m.com.

SIZE UK, 2000.http://www.size.org. (Web site no longer exists).

SIZE USA, 2002.http://www.sizeusa.com.

YI-HSUEH YANG

YI-HSUEH YAN Greceived a M. S. degree from the Department of Industrial Engineering at National Tsing Hua University, Taiwan in 1993 and is engaged in study for a Ph.D. at the same university. His interests are in 3-D anthropometry, occupational biomechanics, and color vision.

CHI-YUANG YU, Ph.D

CHI-YUANG YU, Ph.D., is a graduate of the Department of Industrial and Operations Engineering at the University of Michigan, Ann Arbor in 1988. He is now an associate professor in the Department of Industrial Engineering in National Tsing Hua University, Taiwan. His specialty is occupational biomechanics and color vision. In occupational biomechanics, he has worked on the development of an ergonomics work chair, a 3-D nationwide craniofacial database, and initiating a nationwide anthropometric database survey. Also in color vision, his interests are in uniform color space and color contrast.